Design and implementation of a high-voltage high-frequency pulse power generation system for plasma applications

M. T. Tsai .
Department of Electrical Engineering,
Southern Taiwan University
Tainan, Taiwan, R. O. C.

C. W. Ke
Department of Electrical Engineering,
Southern Taiwan University
Tainan, Taiwan, R. O. C.

***Abstract*—This paper presents a high-voltage high-frequency inverter for atmosphere plasma applications. The proposed system is consisted of a PFC rectifier, a voltage-source full-bridge inverter with phase-shift control, a high-voltage high-frequency transformer, and a plasma reactor. The mathematical models including the inverter and the plasma reactor have been described. The PFC rectifier is achieved by UC3854 based controller, and UC 3895 plus PIC16F877 microcontroller are applying to the inverter. Experimental results show the features of the PWM and PDM control strategies in accordance with the applications**

Keywords: atmosphere plasma; high-frequency; phase-shift control.

I. Introduction

High-voltage high-frequency pulse power supply has been investigated for a long time and is largely industrialized at the fields of semiconductor manufacturing, packing, PCB and LCD panel manufacturing [1-8]. In addition, it is also widely utilized for chemical processing of water and exhausted smoke, and disinfection in industrial pipeline system. It takes advantage of an efficient silent-discharge and is designed for large-scale applications in industrial pipeline plants. However, much progress is still continuous to increase the overall efficiency of existing reactors. In this paper, a high-voltage high-frequency pulse power supply for plasma applications is presented. It is used for the field of gas discharge, including dielectric barrier discharge (silent-discharge) and corona-discharge. The former is the most widely used in industrial large-scale ozone-generation system, and ozone gas can be practically produced on the basis of silent-discharge phenomena. The later is widely used for gas clean system.

The proposed high-voltage high-frequency pulse power supply mainly consists of a PFC rectifier and a voltage-source full-bridge inverter. The inverter out is connected to the load through a high-voltage high-frequency transformer. Pulse-width modulation (PWM) and pulse-density modulation (PDM) have been considered for regulating the output power of the inverter. The PFC rectifier control is achieved by UC3854 based controller. The inverter control is finished by UC3895 controller plus PIC based microprocessor.

II. System configuration

Fig. 1 shows the circuit diagram of the plasma generation equipment. The PFC rectifier is shown in Fig. 1(a), and the resonant inverter is shown in Fig. 1(b). The equivalent circuits of the high-frequency high-voltage transformer and the plasma reactor have also been shown in these figures, where L_r and L_m are corresponding to the leakage inductance and magnetizing inductance of the high-frequency transformer. Since the plasma reactor is connected to the inverter through the high-frequency transformer, the leakage inductance L_r is inserted in series with it. The characteristic of the plasma reactor is greatly dependent on the geometry of the electrode of equipment.

Generally, the discharge gap is modeled as a capacitor before plasma operation and as a direct voltage source connected in parallel with a diode rectifier after plasma operation. The buffer dielectric is modeled as a capacitor. Fig. 2 indicates the status of each interval, where C_e, and C_g exist in the status before plasma operation, and only C_e exists while plasma is generating, V_Z denotes the discharge sustaining voltage.

To estimate these parameters is essential for providing a stable power supply operation. However, these parameters can vary with the change of the gas discharge state of the plasma reactor such as gas composition, inflow gas and the geometry of the electrode [5]. It is difficult to measure directly, but can be estimated on the basis of the Lissajours figure [5, 7-8]. Another way to extract the related parameters of the plasma reactor can been taken from [5], which also pointed out the plasma reactor exhibits two distinct features before and after plasma operation. [8] has provided a good illustration to realize the reactor parameters and power dissipation. Thus, one can see that the inverter resonant frequency during plasma operation should be lower than before plasma operation and the power supply needs to be design in accordance with these changes.

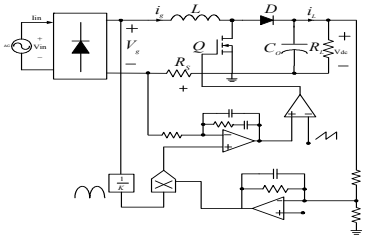

Fig. 1(a). PFC stage control structure.

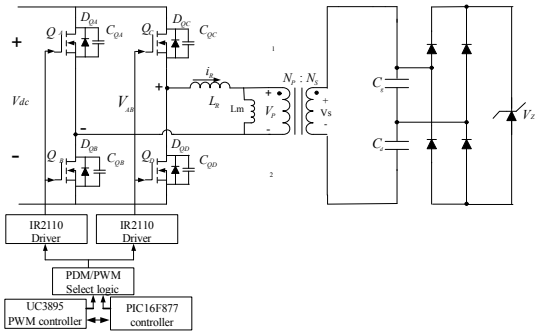

Fig. 1(b). Inverter stage control structure.

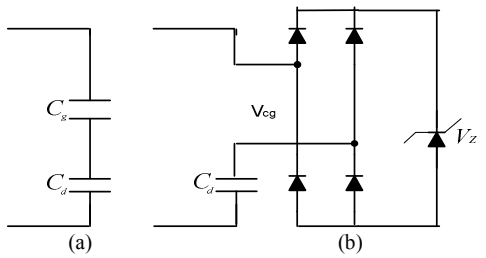

Fig. 2. Reactor model in different operation status, (a) before plasma, (b) plasma operation.

III. CONTROL CIRCUIT

A. PFC stage

The PFC stage uses the UC3854 based average-mode controller to accomplish fixed frequency current control with stability and low distortion. Unlike peak current-mode, average current control accurately maintains sinusoidal line current without slope compensation and with minimal response to noise transients. Fig. 1(a) shows the control structure.

B. Inverter stage

The inverter has five statuses including active and passive determined by the power switching elements of the two legs. The active status is in which two diagonally opposite power switches are conducting. The passive status presents the two switches on the same voltage levels. The leading leg moves the inverter from active status to passive status. The trailing leg moves the inverter from passive status to active. For phase shift control and with the lossless snubbing capacitor, the ZVS can be achieved in the leading leg for all the load conditions, but can be achieved in the trailing leg only in the case that the inverter operates with a lagging load current. For a RLC series circuit, it means the inverter switching frequency should be higher than the load resonant frequency.

The PWM control is achieved by shifting the phase difference of the control phase with respect to the standard phase, while the output power can be varied from full power to low power. Therefore it is feasible to regulate the inverter output power. It should be noted in a discontinuous load case or leading load case, the ZVS function can not be achieved in the trailing leg, resulting in an increasing switching loss. In addition, the inverter output power factor also decreases as the pulse width increases when the switching frequency is constant. A small pulse width tends to a discontinuous load current or leading load current, which is adverse to the switching loss, thus it is disapproved for a low pulse width control. Fig.3 shows the switching relationship of the power elements and the corresponding inverter output voltage and current. Fig. 4 shows the five status of the inverter.

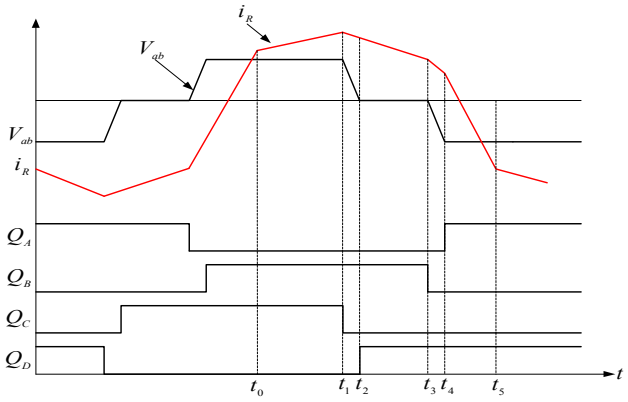

Fig.3. The switching relationship of the power elements and the corresponding inverter output voltage and current.

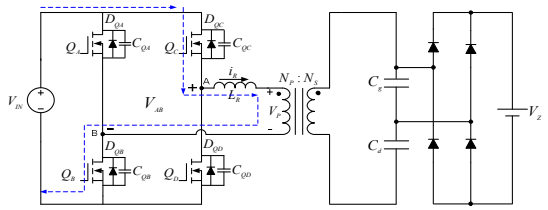

(a)

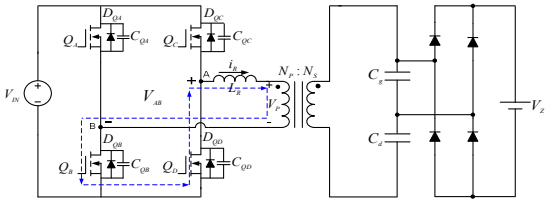

(b)

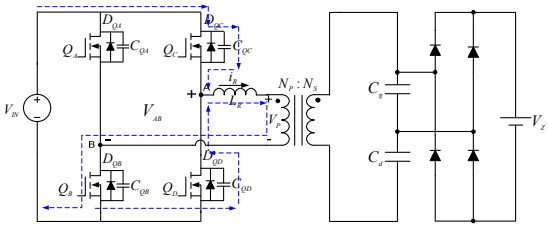

(c)

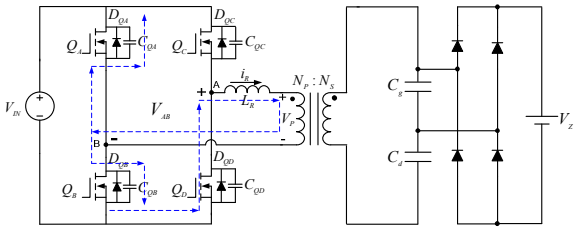

(d)

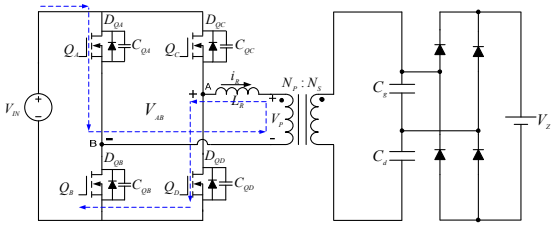

(e)

Fig. 4. The five conducting status of the inverter

The PDM controls the output power by controlling the number of inverter output voltage pulses in accordance with the desired output power. The inverter repeats the gas discharge procedure which consists of power-on period and zero-power period. [1] has shown this method can work well over a range of pulse densities from 3/30 to 1. The PDM scheme can have lower switching loss than other schemes as it achieves quasi-ZCS and ZVS functions [3]. In PDM scheme, the inverter output power maybe varies with the environment temperature fluctuations. Two strategies can be applied in this situation: one is PDM plus PWM based feedback control algorithm [4]; the other is PDM plus PFM based control algorithm [1]. This paper utilizes a UC3895 plus PIC16F877 based hybrid control to realize this control scheme. The PIC16F877 microprocessor determines the control algorithm, and a corresponding control signal is given to the UC 3895 controller and the PDM/PWM select logic circuit. The desired synchronized signal is provided by the UC3895 controller. Fig. 5 shows the proposed synchronized circuit for the PDM control.

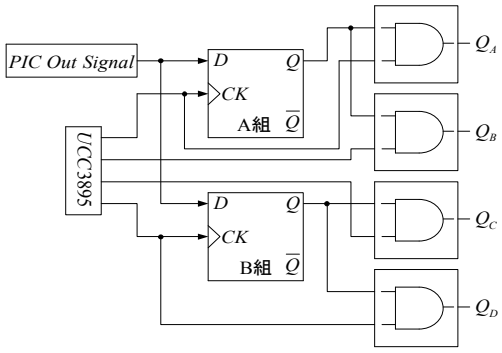

Fig. 5. The proposed synchronized circuit for the PDM control.

A PSIM based simulation has been made to exhibit the plasma reactor characteristic and is shown in Fig. 6. Fig. 6(a) shows the series RLC model, where L_{eq} denotes the equivalent inductor (seen from second side). When the inverter is switching, one can see that it should have two operation states, including corona discharging and not discharging. For the inverter output voltage and frequency at which the value of voltage amplitude on capacitor C_g can not reach the gas discharge value, V_Z , the system has the maximum resonant frequency of $f_{r\max}$. When the inverter output voltage and frequency at which the value of voltage amplitude on capacitor C_g reaches the gas discharge value, V_Z , the system resonant frequency will be reduced to minimum situation of $f_{r\min}$. These two terms can be represented as follows:

$$f_{r\max}=\frac{1}{2\pi\sqrt{L_{eq}C_{eq}}},\quad C_{eq}=\frac{C_gC_d}{C_g+C_d} \tag{1}$$

$$f_{r\min}=\frac{1}{2\pi\sqrt{L_{eq}C_d}}, \tag{2}$$

The value of V_S can be shown as follows;

$$V_{S1}=\frac{4}{\pi}V_{dc}\frac{N_S}{N_P}\cos\frac{\mu}{2}, \tag{3}$$

Thus, the voltage at the capacitor C_g can be obtained as follows:

$$\frac{V_{cg}}{V_S}=\frac{-1}{\omega^2L_{eq}C_dC_g-(C_d+C_g)}C_d=\frac{-1}{(\omega^2L_{eq}C_Z-1)}\frac{C_Z}{C_g},\qquad C_Z=\frac{C_dC_g}{C_d+C_g}, \tag{4}$$

Assuming V_Z as the gas discharge starting voltage, then the switching boundary frequencies at which gas discharge starts can be obtained as follows[8]:

$$f_{S\max}=\frac{1}{2\pi}\sqrt{\frac{1}{L_{eq}C_d}(\frac{C_d}{C_Z}+\frac{V_S}{V_Z})}=\frac{1}{2\pi}\sqrt{\frac{1}{L_{eq}C_d}(\frac{C_d}{C_Z}+\frac{4}{\pi}\frac{V_{dc}}{V_Z}\frac{N_S}{N_P}\cos\frac{\mu}{2})}, \tag{5}$$

The switching frequency of the inverter should meet the above equations, and $f_{S\max}$ is dependent on the parameters including transformer, plasma reactor, and the values of the inverter input voltage and the inverter output pulse-width. Fig. 6(b)-(d) depict an example of waveforms of voltage and charge on plasma reactor.

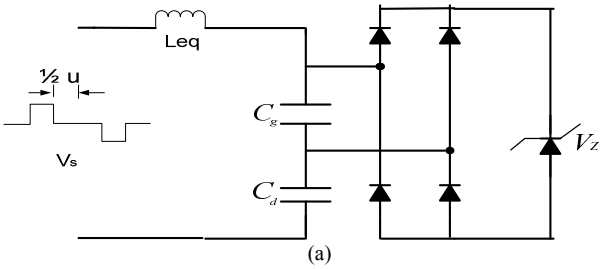

(a)

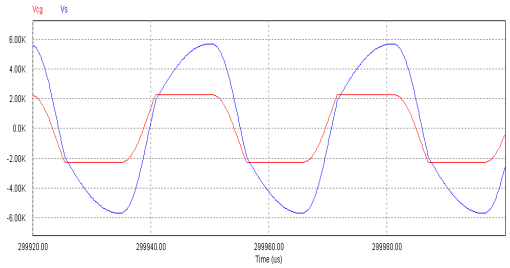

(b)

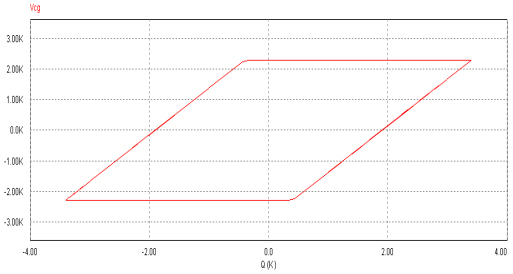

(c)

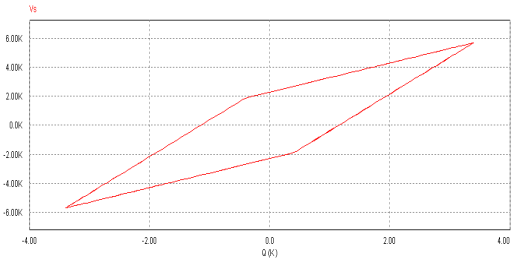

(d)

Fig. 6. PSIM based simulation for plasma reactor characteristic, (a) system model, (b) plasma reactor input voltage and gas discharger, (c) gas discharge voltage verse charger, (d) plasma reactor input voltage verse charger.

IV. EXPERIMENTAL RESULT

Figure 7 shows the experimental results for the PFC stage. Fig. 7(a) shows the source voltage and current for a load case of 500W; Fig. 7(b) shows the source voltage and current for a load case of 1000W. It shows the source current has in-phase with the source voltage.

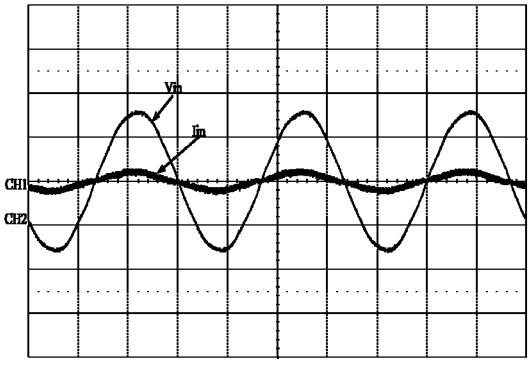

CH1-20A CH2-200V M-5ms/div

Fig. 7(a). The source voltage and current for a load case of 500W

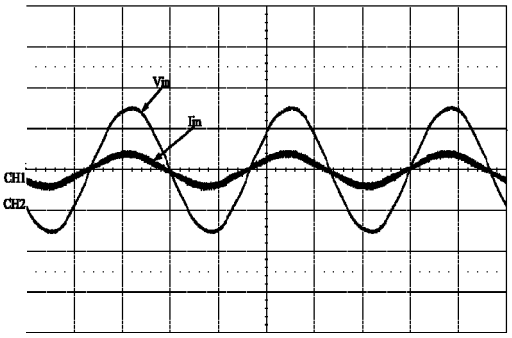

CH1-20A CH2-200V M-5ms/div

Fig. 7(b). The source voltage and current for a load case of 1000W

Figure 8 shows the experimental result of PWM based control scheme. Fig. 8(a) shows a case of 50% pulse width duration. Fig. 8(b) shows a case of 75% pulse width duration. Fig. 8(c) shows a case of 50% pulse width duration. It shows the inverter output power increases as the pulse width increases, and the power factor decreases as the output power increases. The input power related to there figures are 470W, 630W and 720W. The switching frequency used here is 40 kHz.

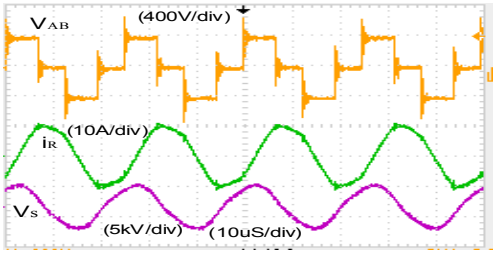

(a)

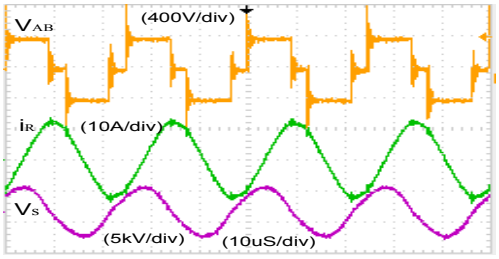

(b)

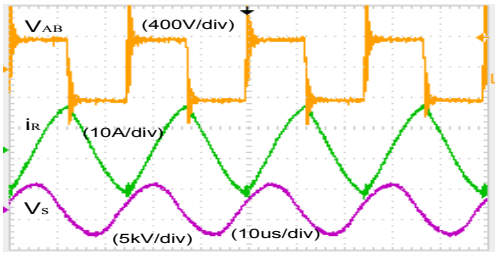

(c)

Fig. 8. The experimental results of PWM control at 40 kHz switching frequency.

Fig. 9 shows an experimental result of ZVS switching case for the inverter. Fig. 9(a) shows the leading leg situation. Fig. 9(b) shows a similar result for the lagging leg.

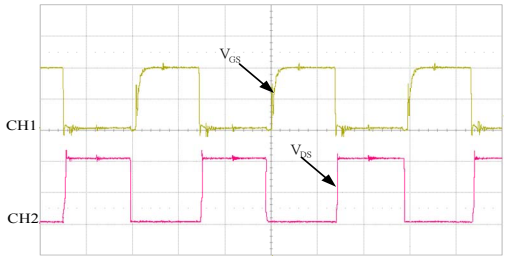

(a)

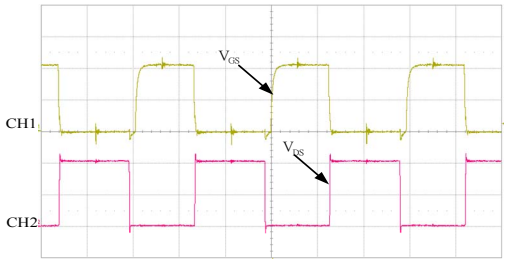

(b)

Fig. 9. ZVS switching case for the inverter

Figure 10 shows the experimental waveforms of PDM based control scheme. Fig. 10(a) shows the case of operation at a pulse density of 25% (10/40). The input power is about 230W. Fig. 10(b) shows the case of operation at a pulse density of 50% (20/40). The input power is about 420W. The switching frequency in this cases are about 40 kHz. It shows the inverter output power increases as the pulse density increases.

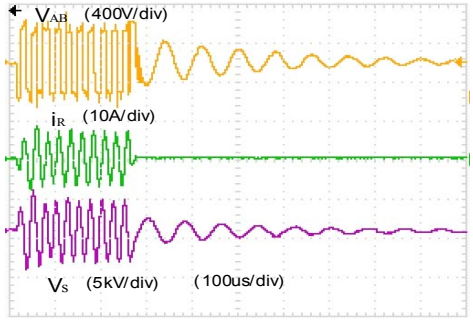

(a)

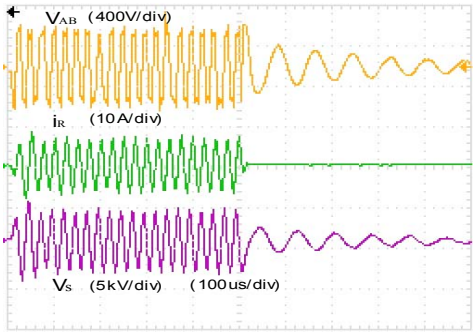

(b)

Fig. 10. The corresponding waveforms for PDM control .

V. Conclusion

In this study, a high-voltage high-frequency power supply for atmosphere plasma applications has been presented. The PWM and PDM control strategies have been tested to evaluate the power control effect. As the experimental results, these two control strategies can fulfill the full load range conditions. However, a small pulse width tends to a discontinuous load current which is adverse to the switching loss, thus it is disapproved for a low pulse width control for the PWM strategy. By the way, the environment temperature fluctuations can disturb the stability of the inverter output power for the PDM control. To compensate this influence, a hybrid control such as PDM plus PFM or PDM plus PWM is suggested.

Acknowledgment

This work was supported by Technology Development Program for Academia, Ministry of Economic Affairs, R. O. C. under research project 98-EC-17-A-05-S2-0061.

References

1. Y. Liu, X. He, " PDM and PFM hybrid control of a series-resonant inverter for corona surface treatment, " IEE Proc.-Electr. Power Appl. Vol. 152, no.6, pp. 1445-1450, November 2005.
2. J. Marcos, J. Cardesin, E. L. Corominas, R. Secades, and J. Carcia, " Low-power high-voltage high-frequency power supply for ozone generation," IEEE Transactions on Industry Applications, vol. 40, no. 2, pp. 414-421, March/April, 2004.
3. H. Fujita, H. Akagi, " Control and performance of a pulse-density-modulated series-resonant inverter for corona discharge processes, "IEEE Transactions on Industry Applications, vol. 35, no. 3, pp. 621-627, May/June, 1999.
4. O. Koudriavtsev, S. Wang, Y. Konishi, and M. Nakaoka, " A novel pulse-density-modulated high-frequency inverter for silent-discharge-type ozonizer, " IEEE Transactions on industry applications, vol. 38, no. 2, pp. 369-378, March/April, 2002.
5. Y. D. Lee, W. C. Lee, T. K. Lee, " A study on the reactor parameter of atmosphere plasma power supply, " IEEE Power Electronics and Applications, 2007 European Conference, pp. 1-8, Sept. 2007.
6. Y. M. Kim, J. Y. Kim, S. P. Mun, H. W. Lee, S. K. Kwon, K. Y. Suh, " The design of inverter power system for plasma generator," IEEE Electrical Machines and Systems, pp. 1309-1312, 2005.
7. R. Feng, G. S. P. Castle, S. Jayaram, " Automated system for power measurement in the silent discharge, "IEEE Transactions on Industry Applications, vol. 34, no. 3, pp. 563-570, May/June, 1998.
8. M. Jan, " Corona treatment system with resonant inverter-selected proprieties," 2008 13th International Power Electronics and Motion Control Conference (EPE-PEMC 2008), pp. 1316-1320, 2008.